Morphometric fingerprint of asymptomatic *Parkin* and *PINK1* mutation carriers in the basal ganglia

F. Binkofski, MD*

K. Reetz, MD*

C. Gaser, PhD

R. Hilker, MD

J. Hagenah, MD

K. Hedrich, PhD

T. van Eimeren, MD

A. Thiel, MD

C. Büchel, MD

P.P. Pramstaller, MD

H.R. Siebner, MD

C. Klein, MD

Address correspondence and reprint requests to Dr. Ferdinand Binkofski, Department of Neurology, University Hospital Schleswig-Holstein, Campus Luebeck, Ratzeburger Allee 160, 23538 Luebeck, Germany ferdinand.binkofski@neuro.uni-luebeck.de

ABSTRACT

Background: Mutations in the *Parkin* and *PINK1* genes can cause parkinsonism. Since asymptomatic carriers of a single mutant allele of the *Parkin* or *PINK1* gene display a presynaptic dopaminergic dysfunction in the striatum, they provide a unique in vivo model to study structural and functional reorganization in response to latent nigrostriatal dysfunction. We hypothesized that subclinical nigrostriatal neurodegeneration caused by these mutations would induce morphologic changes in the dysfunctional striatal gray matter.

Methods: In asymptomatic carriers of a heterozygous *Parkin* (n = 13) or *PINK1* (n = 10) mutation and 23 age-and sex-matched individuals without a mutation, we applied observer independent region-of-interest and voxel-based morphometry to high-resolution structural MRIs.

Results: Relative to controls without a mutation, *Parkin* and *PINK1* mutation carriers displayed a bilateral increase in gray matter volume in the putamen and the internal globus pallidus. In 8 of the 13 *Parkin* mutation carriers, the presynaptic dopaminergic function was studied with ^{18}F-DOPA PET. The metabolic-morphometric regression analysis revealed that the linear decrease in individual presynaptic striatal ^{18}F-DOPA uptake was linked to a reciprocal decrease in the striatal gray matter volume in the putamen bilaterally and in the left caudate nucleus.

Conclusions: The alternative causes of the increased striatal gray matter volume may be either due to excessive levels of neuronal activity caused by chronic dopaminergic dysfunction or due to long-term adaptation to chronic nigrostriatal dysfunction actively compensating for the dopaminergic denervation. In any case, the results indicate that a genetically driven regional dysfunction may be imprinted in the structure of the dysfunctional brain region, for example in the striatum.
Neurology® **2007;69:842–850**

There is little knowledge about in vivo changes in the human brain prior to the onset of Parkinson disease (PD). Clinical symptoms of PD are preceded by a substantial neurodegeneration of dopamine-producing neurons in the substantia nigra, causing a marked reduction of dopamine uptake in the striatum, especially in the posterior putamen. This indicates a great potential of the brain to compensate for progressive nigrostriatal degeneration over an as yet unknown time period.[1] Elucidating the presymptomatic period and the mechanisms that underlie potential compensation in humans is of major importance for a better understanding of the development of neurodegenerative disorders such as PD.

In nonhuman primates, chronic administration of N-methyl-4-phenyl-1,2,3,6-tetrahydropyridine (MPTP), that produces subacute striatal dopaminergic denervation,

induced several compensatory mechanisms within the cortical-basal ganglia-thalamocortical circuitry that counteracted the functional consequences of dopaminergic denervation during the presymptomatic period of MPTP-induced parkinsonism.[2] These compensatory mechanisms appear to act independently and are able to actively delay the occurrence of symptoms of parkinsonism.

An elegant way to investigate presymptomatic mechanisms in humans is to study a group of asymptomatic individuals who carry mutations in genes that are associated with parkinsonism. Mutations in the *Parkin* gene are the most common known single factor responsible for early onset parkinsonism, followed by mutations in the *PINK1* gene.[3] Mutations in these two genes can lead to a phenotype indistinguishable from that of idiopathic PD.[3-7] However, the similarities between *Parkin*- and *PINK1*-associated parkinsonism and idiopathic PD extend far beyond the clinical picture: for example, postmortem analysis of the index patient of a large *Parkin* pedigree (Family LA) revealed classic idiopathic PD-like findings including alpha-synuclein-positive Lewy bodies.[8]

Of note, asymptomatic carriers of a single mutant *Parkin* or *PINK1* allele also display a latent abnormality of striatal dopaminergic function as revealed by ^{18}F-DOPA PET.[9,10] ^{18}F-DOPA PET findings in asymptomatic carriers of a single mutant *Parkin* allele from the Family LA revealed a reduction of ^{18}F-DOPA uptake in the posterior dorsal putamen.[9-13] Additional changes in brain structure and function have been found using transcranial sonography and functional MRI (fMRI) in asymptomatic individuals who carry a mutant *Parkin* or *PINK1* allele. Transcranial sonography revealed hyperechogenicity of the substantia nigra in both symptomatic and asymptomatic *Parkin* mutation carriers,[14] a finding that can also be detected in most patients with idiopathic PD. Our recent fMRI study[15] showed changes in movement-related neural activity in the motor system which were attributed to a compensatory reorganization within the striatocortical motor loops to counterbalance the latent nigrostriatal dysfunction.[15] Taken together, asymptomatic carriers of a single mutant *Parkin* or *PINK1* allele provide a unique in vivo model to study structural and functional consequences of latent nigrostriatal dysfunction using neuroimaging.[16]

The present morphometric study addressed the question as to whether the latent nigrostriatal dysfunction caused by a mutation in the *Parkin* or *PINK1* gene alters the gray matter volume in the human striatum of asymptomatic carriers of a single mutant allele. To this end, asymptomatic mutation carriers and healthy controls without a mutation underwent high-resolution structural MRI. We applied observer independent region of interest (ROI)-based and voxel-based morphometry (VBM) to investigate how a chronic nigrostriatal dopaminergic deficit shapes the structure of the human striatum without causing overt disease. In eight asymptomatic *Parkin* mutation carriers, we were also able to search for a direct relationship between the striatal dopaminergic deficit and the structural changes in this region, since we had access to their ^{18}F-DOPA PET data.[17]

METHODS **Subjects.** We studied 13 asymptomatic heterozygous *Parkin* mutations carriers (five male, eight female, mean age: 39.6 years [±5.6]) and 10 asymptomatic heterozygous *PINK1* mutation carriers (eight male, two female, mean age: 42.7 years [±5.7]). All mutation carriers were members of two large families. Members of Family LA either carried a heterozygous deletion of exon 7 or a heterozygous single base-pair deletion (c.del1072T) in exon 9 of *Parkin*.[8] Members of Family W were heterozygous carriers of the recurrent c.1366C>T stop mutation in the *PINK1* gene.[18] Two of the asymptomatic heterozygous *Parkin*[8] and six of the *PINK1* mutation carriers[5] had minor motor signs upon careful clinical examination but were unaware of these signs. In addition, we investigated 23 age- and sex-matched healthy volunteers without mutations in the *Parkin* or *PINK1* gene (13 male, 10 female, mean age: 41.1 years [±8.4]). All volunteers had a normal neurologic and neuropsychological examination. There was no age difference between these groups ($p = 0.95$, two-tailed t test).

All subjects gave written informed consent for participation in this study which was approved by the local ethics committee.

Structural MRI scanning. Scanning was performed with a 1.5 T whole-body scanner (Siemens, Symphony, Erlangen,

Germany). All subjects underwent structural MRI using a T1-weighted FLASH three-dimensional MR sequence (echo time [TE] = 5 msec; repetition time [TR] = 15 msec; flip angle = 30°; isotropic voxel size $1 \times 1 \times 1$ mm³).

Morphometric analysis was performed on a voxel-by-voxel basis using SPM2 software (Wellcome Dept. of Imaging Neuroscience, Institute of Neurology, UCL, London, www.fil.ion.ucl.ac.uk/spm). VBM was complemented by conventional ROI-based morphometry.

Morphometric analysis. The spatial normalization to the standard anatomic space was performed in a two-stage process. In the first step, we registered each image to the template of the International Consortium for Brain Mapping (Montreal Neurological Institute, Montreal, Canada), which approximates Talairach space. We applied a 12-parameter affine transformation to correct image size and position. Regional volumes were preserved, while corrections for global differences in whole brain volume were made. The normalized images of all subjects and patients were averaged and smoothed with a Gaussian kernel of 8 mm full-width at half maximum (FWHM). Using the optimized procedure,[19] these normalized images were used to create a new template with reduced scanner- and population-specific bias. In the second normalization step, we locally deformed each image of our entire group to the new template using a nonlinear spatial transformation. This accounts for the remaining shape differences between the images and the template, and improves the overlap of corresponding anatomic structures. Using a modified mixture model cluster analysis, normalized images were corrected for non-uniformities in signal intensity and partitioned into gray and white matter, CSF, and background. To remove unconnected non-brain voxels (e.g., rims between brain surface and meninges), we applied a series of morphologic erosions and dilations to the segmented images.[19]

VBM-based analysis. Images were smoothed with a Gaussian kernel of 12 mm FWHM. We employed a voxel-by-voxel one-way analysis of variance to test for differences in gray matter volume between groups. An absolute gray matter threshold of 0.25 was applied to avoid possible edge effects around the border between gray and white matter or CSF. Linear contrasts were specified to quantify relative differences in gray matter volume between each group of asymptomatic mutation carriers and their corresponding control group without mutation. The statistical threshold was set at $p < 0.01$. The localization of the cluster within specific basal ganglia structures was accessed by taking reference to published coordinates.[13,20] Given our a priori hypothesis, we applied a small-volume correction (SVC), using a sphere of 10 mm radius and corrected for multiple comparisons using the false discovery rate (FDR) method as implemented in SPM2.

ROI-based analysis. We also performed ROI-based morphometry using the same structural MRI data set in the reference brain and integrated the gray matter values of each brain in these ROIs. The ROIs were derived from the Anatomic Automatic Labeling atlas (AAL),[21] an automated parcellation method,[21] included in the WFU-Pickatlas SPM toolbox,[21,22] and we used the putamen and the globus pallidus masks in each hemisphere to calculate the volumes for each subject. The ROI-based morphometric approach enabled us to calculate the number of voxels and volumes of single structures in the basal ganglia supporting the comparison with other conventional volumetric studies.

Linking striatal structure to regional dopaminergic function. Eight asymptomatic heterozygous *Parkin* mutation carriers had previously undergone ¹⁸F-DOPA PET measurements. Details of the ¹⁸F-DOPA PET measurements are described elsewhere.[9] In these mutation carriers, we performed a voxel-by-voxel simple regression analysis to test for a linear relationship between individual gray matter images and the ¹⁸F-DOPA influx constants (Ki values) from the posterior putamen and caudate. For the regression analysis, individual integrated images of dynamic time frames constructed over a 24.5 to 94.5 minute epoch from injection of ¹⁸F-DOPA were taken. Ki values were calculated graphically from 24.5 to 94.5 minutes after injection using an occipital reference region input function.[23] In each individual, ROIs were defined in the posterior putamen and in the caudate using the MRICRO software to obtain individual Ki values in these regions. These subject-specific Ki values were then used as a regressor to identify in a voxel-by-voxel correlation brain areas in which gray matter volume is correlated with ¹⁸F-DOPA uptake. We reasoned that neurodegeneration of the dopaminergic nigrostriatal projections should primarily induce morphometric changes in the dysfunctional basal ganglia, and that these changes should correlate with the magnitude of presymptomatic dopaminergic striatal dysfunction.

RESULTS VBM revealed that the presence of a heterozygous mutation, irrespective of the genotype (i.e., mutant allele of the *Parkin* or *PINK1* gene), was associated with a bilateral increase in gray matter volume in the posterior putamen and in the GPi (table 1, figure, A. Direct comparisons of *Parkin* or *PINK1* mutation carriers with their corresponding control groups showed that the gray matter increase was comparable for both genotypes. In asymptomatic heterozygous carriers of *Parkin* mutations, VBM disclosed a bilateral significant increase in gray matter volume in the posterior putamen that was accentuated on the left side. Peak changes in gray matter volume were found in the left posterior putamen and in the right putamen. An increase in gray matter volume was also revealed in the left globus pallidus internus (GPi) (table 1). A similar pattern emerged in asymptomatic heterozygous carriers of a *PINK1* mutation. The presence of a mutant *PINK1* allele was associated with an increase in gray matter volume in the left and right posterior putamen (table 1).

ROI-based morphometry confirmed the VBM findings (table 2). Asymptomatic heterozygous *Parkin* mutation carriers showed a bilateral increase in mean gray matter volume of the putamen relative to controls without mutations (table 2). The volume of the pallidum was only increased on the left side compared with controls.

Table 1 — Voxel-based morphometry MNI coordinates and morphometric-metabolic regression

Region	Side	MNI coordinates in mm			Z-score	p_FDR-corr SVC
		x	y	z		
Increase in gray matter volume						
Asymptomatic *Parkin* and *PINK1* mutation carriers > controls						
Putamen	L	−25	−7	0	3.09	0.018
Putamen	R	28	−3	−5	3.08	0.010
GPI	L	−22	−4	0	3.11	0.018
GPI	R	14	1	−6	2.23	0.021
Asymptomatic *Parkin* mutation carriers > controls						
Putamen	L	−22	−5	4	2.86	0.021
Putamen	R	29	−8	−8	2.68	0,032
GPI	L	−15	−5	−8	3.07	0.017
GPI	R	—	—	—	—	—
Asymptomatic *PINK1* mutation carriers > controls						
Putamen	L	−32	1	−6	2.70	0.046
Putamen	R	28	0	−5	3.03	0.023
GPI	L	—	—	—	—	—
GPI	R	—	—	—	—	—
Simple regression analysis between gray matter volume and Ki values in asymptomatic *Parkin* mutation carriers						
Caudate	L	−13	3	5	3.39	0.017
Caudate	R	—	—	—	—	—
Putamen	L	−17	1	4	3.61	0.026
Putamen	R	23	−4	−2	3.15	0.026
GPI	L	−19	−8	0	3.93	0.005
GPI	R	19	−6	−1	3.77	0.038

SVC = small volume correction; GPI = globus pallidus internus; Ki = ^{18}F-DOPA influx constant.

In asymptomatic heterozygous PINK1 mutation carriers, ROI-based morphometry revealed a significant increase in gray matter volume of the right putamen and a trend toward increased putaminal volume on the left side. In addition, the presence of a mutant *PINK1* allele was associated with a bilateral increase in mean gray matter volume in the pallidal ROI.

In the eight asymptomatic heterozygous *Parkin* mutation carriers who had undergone ^{18}F-DOPA PET, simple regression analysis between the individual presynaptic striatal ^{18}F-DOPA uptake and the morphometric data revealed that the striatal Ki values decreased linearly and were linked to a reciprocal increase in the gray matter volume in the striatum (table 1, figure, B). This was the case in left posterior putamen (table 1; R = 0.93, R^2 = 0.87), right posterior putamen (R = 0.96, R^2 = 0.92), and the head of left caudate nucleus (R = 0.90, R^2 = 0.80). Individual striatal Ki values showed a linear decrease with increasing gray matter volume in the GPi bilaterally.
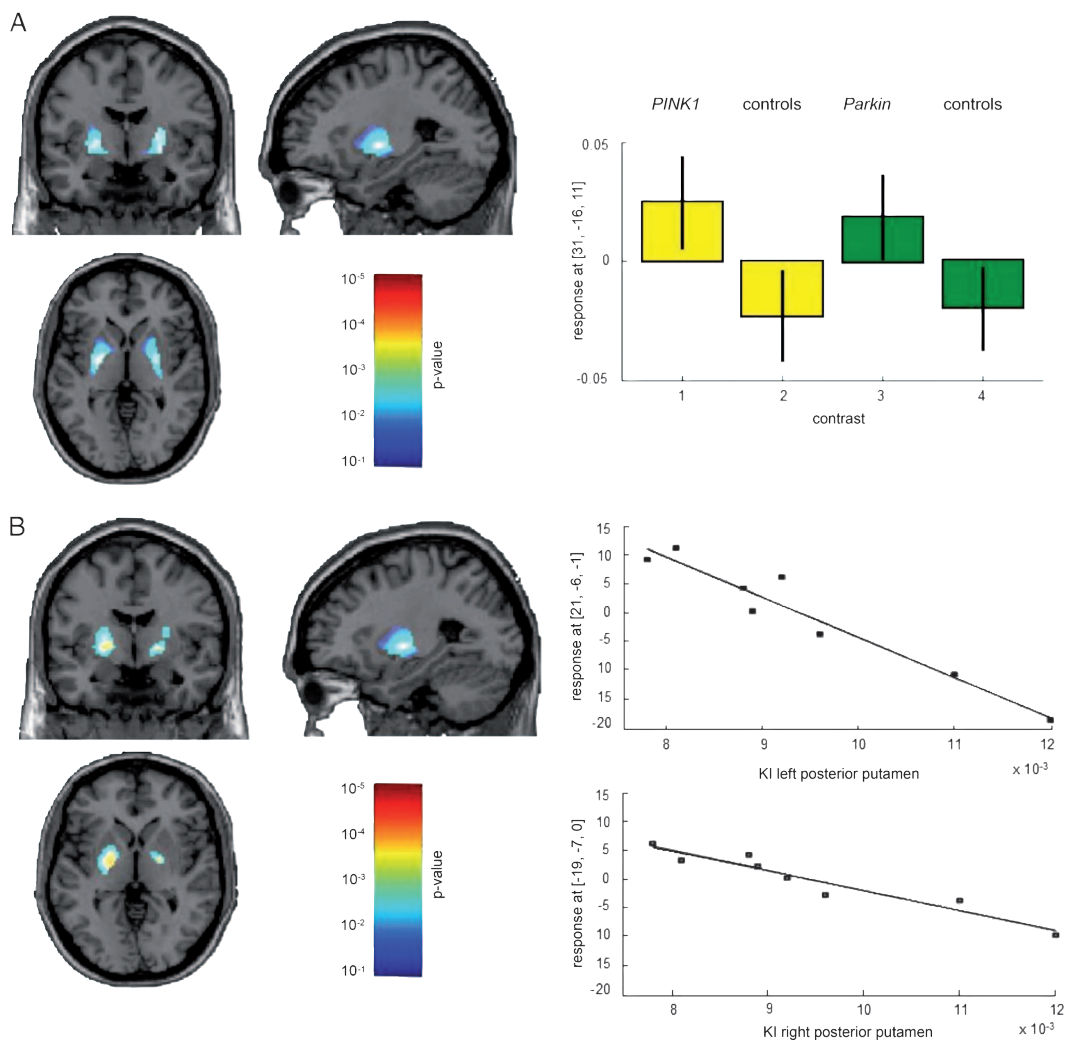
Of note, using VBM with the same statistical criteria as above an increase in gray matter volume in small cortical areas has also been found within the right inferior frontal gyrus, left insula, and bilateral superior and inferior temporal gyri in both groups of mutation carriers. But since we focused on the motor system, relevant motor areas will further be emphasized.

DISCUSSION Observer independent voxel-based and ROI-based analysis of striatal gray matter provided converging evidence that the presence of a single mutant allele in the *Parkin* or *PINK1* gene leads to a bilateral increase in gray matter in the posterior putamen and GPi. In a subgroup of asymptomatic heterozygous *Parkin* mutation carriers, who had been examined with ^{18}F-DOPA PET, striatal gray matter volume was inversely related with the regional Ki values. The higher the regional reduction in striatal dopamine uptake, the greater the regional increase in gray matter volume.

We highlight the converging effects of heterozygous carriers of mutations in two parkin-

Figure Striatal changes in gray matter volume in asymptomatic carriers of a single mutant *Parkin* or *PINK1* allele and metabolic-morphometric regression analysis

(A) Main contrast between the VBM data of the asymptomatic heterozygous *Parkin* and *PINK1* mutation carriers and matched controls without a *Parkin* or *PINK1* mutation revealing an increase of the volume of the striatum and GPI in both groups. The left panels show the statistical parametric maps thresholded at 0.01. The right panels give the parameter estimates of the gray matter values of asymptomatic heterozygous *Parkin* and *PINK1* mutation carriers and controls in the posterior putamen. (B) Simple regression analysis between the individual gray matter images of eight asymptomatic heterozygous *Parkin* mutation carriers and the individual Ki values, obtained from the posterior putamen at the voxel-by-voxel level. The Ki values showed a linear decrease with increasing gray matter volume mainly in the left posterior putamen and to a lesser extent in the right putamen. The color scale represents the *p* values. A basal ganglia mask obtained from the WFU-PickAtlas (ANSIR, Wake Forest University)[22] was used for anatomic visualization.

sonism genes and introduce two alternative hypotheses (dysfunctional hypertrophy vs active compensation) which provide a possible explanation for the striatal hypertrophy and the individual PET Ki values decreasing reciprocally with the increasing gray matter volume in the striatum.

^{18}F-DOPA uptake in the striatum reflects the volume of striatal dopaminergic terminals and the conversion of ^{18}F-DOPA to ^{18}F-dopamine, and its storage, measuring the presynaptic dopaminergic function. Reduction of ^{18}F-DOPA uptake in the posterior putamen contralateral to the initially affected limb is one of the first findings in patients with early idiopathic PD.[9] It is worth noting that

^{18}F-DOPA overestimates the number of striatal dopaminergic nerve terminals in the early stage of PD because an increased dopamine turnover in the surviving terminals partially compensates for the loss of dopaminergic synapses.[24] Therefore, the slight, albeit significant, reduction of ^{18}F-DOPA uptake in the posterior putamen found in the asymptomatic heterozygous carriers of *Parkin* and *PINK1* mutations[9,25] only represents the tip of the iceberg of a larger underlying damage of the dopaminergic terminals. Indeed, it was recently demonstrated in four asymptomatic carriers of *LRRK2* mutations causing dominant PD that ^{18}F-DOPA uptake remained normal, whereas mem-

Table 2		Region of interest–based morphometry in asymptomatic *Parkin* and *PINK1* mutation carriers vs controls		
Region	Side	Mean volume in mm³ * 10³/SD		p Values
		Parkin	Controls	
Putamen	L	5,198 ± 0.206	4,967 ± 0.301	0.021
Putamen	R	5,462 ± 0.206	5,228 ± 0.389	0.008
Pallidum	L	376 ± 88	297 ± 59	0.001
Pallidum	R	430 ± 63	404 ± 84	NS
		PINK1	Controls	
Putamen	L	5,022 ± 0.287	4,796 ± 0.385	NS
Putamen	R	5,427 ± 0.286	5,062 ± 0.482	0.023
Pallidum	L	363 ± 75	309 ± 66	0.041
Pallidum	R	475 ± 100	400 ± 71	0.029

brane dopamine transporter (DAT) binding was deficient in all four and vesicular monoamine transporter binding was abnormal in two of them.[26] These findings seem to confirm the logical conjecture that increased dopamine turnover is present in as yet intact nerve terminals before the manifestation of clinical symptoms.

Given the well-known latent nigrostriatal dysfunction in asymptomatic mutation carriers, we infer that the morphometric changes resulted from the presynaptic dopaminergic deficit in the striatum. This hypothesis is supported by the results of the metabolic-morphometric regression analysis which revealed that the individual Ki values in the striatum decreased linearly with the regional increase of gray matter volume in asymptomatic heterozygous *Parkin* mutation carriers. The compensatory increase in dopamine turnover is energy-consuming and might induce changes in the macrostructure of the striatum, for example through increase in glia[27] and sprouting of vessels. The hypothesis that nigrostriatal dysfunction drives the morphometric change is further supported by a morphometric study on chronic treatment with neuroleptics.[28] This study has shown that the chronic intake of typical neuroleptics binding to D2-receptors leads to a relative increase of basal ganglia volume over a time period of 2 years.[28] After withdrawal of typical neuroleptics, this striatal hypertrophy was reversible.[28]

The increase in striatal gray matter in asymptomatic *Parkin* or *PINK1* mutation carriers may be a long-term consequence of abnormal striatal neuronal activity resulting from the latent nigrostriatal dysfunction.

In a classic model it has been proposed that, during action, there is specific enhancement of activity in corticostriatal loops involved in the cur-rently performed task with concomitant suppression of competing motor networks.[29] This has been suggested to originate from a neuroanatomic arrangement of the corticostriatal system in a center-surround inhibitory pattern.[30] There is evidence that dopamine modulates this corticostriatal activity by enhancing transmission at active synapses while suppressing it at inactive ones,[31] and also by regulating long-term potentiation and depression.[32] Therefore, the effect of dopamine release in the vicinity of highly active corticostriatal terminations could be to increase the signal-to-noise ratio by strengthening that synapse while suppressing neighboring ones. In another model the main action of dopamine in the basal ganglia is hypothesized to regulate the coupling level between the different basal ganglia subcircuits.[33] In the normal state dopamine endings on striatal spines can reduce the efficacy of divergent glutaminergic inputs to the striatum thereby suppressing cross-talk between different afferent channels. Following dopamine depletion the segregation between the afferent channels is lost, resulting in synchronized activation of pallidal cells.[33,34] This model also emphasizes that dimensionality reduction of the corticostriatal neuronal input is an important feature of neuronal processing within the basal ganglia.[35] According to a recent model, the activity of the thalamus and cortex is dynamically controlled through the cortico-nucleus subthalamicus [STN]-GPi hyperdirect, direct, and indirect pathways and releases only the selected motor program at the selected timing, thus extracting the relevant information.[36] According to this model, the pathophysiology of basal ganglia disorders and the mechanism for the effectiveness of functional neurosurgery or stimulation can be explained by an increase or decrease

in disinhibition and inhibition in the thalamus and cortex in the temporal and spatial domains.[36]

Independently of the preferred basal ganglia model, experimental studies of neuronal firing in both humans with PD and animal models of PD provide evidence for an increase in oscillatory activity in the external and internal segments of the globus pallidus (GPi and GPe), and the STN.[37,38] For example, perioperative recordings of oscillatory local field potentials (LFP) in the subthalamic nucleus and globus pallidus in patients with advanced PD revealed abnormal oscillatory activity at 8 to 35 Hz[39] which may be caused by the decreased dopamine uptake. Thus, this activity was prominent when patients with PD had been withdrawn from their dopaminergic medication, which had antikinetic properties, and adversely affected motor processing. Of importance, dopaminergic treatment, behaviorally relevant stimuli, and voluntary movement suppress this abnormal activity. Therefore, it has been proposed that the overexpression of this oscillatory activity contributes to the bradykinesia in symptomatic PD.[40]

For that reason it is conceivable that the latent dopaminergic deficit in our asymptomatic *Parkin* and *PINK1* mutation carriers causes abnormal oscillatory activity in the basal ganglia in the 8 to 30 Hz range. Therefore, the abnormal striatal overactivity related to latent dopaminergic dysfunction in our asymptomatic heterozygous mutation carriers may have resulted in a long-term increase in striatal gray matter.

Examples of dysfunctional structural hypertrophy have been described previously. The classic example is hypertrophy of the inferior olivary nucleus in palatal tremor.[41] This hypertrophic degeneration of the inferior olives appears after disruption of the GABAergic dentato-olivary pathway[41] which causes an abnormal synchronous oscillation of neurons in the inferior olive. This abnormal rhythm interferes with physiologic regulations of the oculomotor and cerebello-reticular systems producing the hyperkinesia of brainstem-innervated muscles and the cerebellospinal systems regulating muscle tone.[41]

The striatal increase in gray matter volume may also be driven by compensatory mechanisms. This hypothesis is supported by recent work in a primate model of PD that produces subacute striatal dopaminergic denervation through chronic MPTP administration. This work revealed several compensatory mechanisms within the cortical-basal ganglia-thalamo-cortical circuitry counteracting the functional consequences of dopaminergic denervation in the presymptomatic

period of MPTP-induced PD.[2] One active presymptomatic compensatory mechanism identified is the upregulation of postsynaptic D2 receptors in the striatum compensating for the breakdown of the striatal dopamine homeostasis.[2] More importantly, multiunit electrophysiologic recordings in monkeys revealed increases in neuronal activity in the GPi and the STN that occurred already within 2 weeks after MPTP injection in the presymptomatic stage and were temporarily uncoupled from the breakdown of dopamine homeostasis in the basal ganglia[2] supporting its compensatory character.

Our recent fMRI study that examined movement-related activity in the same group of asymptomatic heterozygous *Parkin* mutation carriers as in the present study also supports a compensatory mechanism as underlying source of the morphometric changes.[15] Asymptomatic mutation carriers displayed an increased coupling between activity in the anterior cingulate motor area and the left posterior putamen during the performance of internally guided movements. Therefore, we suggest that presynaptic dopaminergic dysfunction in the posterior putamen in asymptomatic carriers of heterozygous *Parkin* mutations leads to a chronic increase in neuronal activity within the basal ganglia and an increase in gray matter volume of the hyperactive structures. This increase in volume might represent a long-term consequence of adaptive plasticity in the basal ganglia that allows for a compensation of the presymptomatic dopaminergic deficit in the striatal motor circuit counteracting imminent motor dysfunction.

We can only speculate about the microstructural changes underlying the expansion in gray matter at the macrostructural level. At the cortex level there is converging evidence that long-term increase in regional activity expands the volume of the active region. Regional cortical hypertrophy has been observed in rat motor cortex following a prolonged period of motor training.[42] A possible mechanism of this cortical thickening might be an increased synaptogenesis.[43,44] In addition, long-term learning processes seem to involve slowly evolving mechanisms, such as neuronal and glial cell genesis.[27] In keeping with this observation, an increase of cortical gray matter in temporo-occipital structures related to long-term visuomotor learning and extensive knowledge acquisition has recently been found in humans.[45,46]

The final question arises why *Parkin* and *PINK1* mutations exhibit similar morphometric changes in the basal ganglia. Heterozygous muta-

tions in the *Parkin* [47] and also in the *PINK1* gene[7] are supposed to act as a susceptibility factor for PD in humans. The clinical picture,[3-5] the histopathologic[8] metabolic PET,[9,10,13] functional fMRI,[15] and structural ultrasound findings[14] in *Parkin* and *PINK1* mutation carriers have consistently supported the pathogenic effect of heterozygous mutations in these genes. Here we investigated for the first time gray matter volume at the structural level in asymptomatic heterozygous *Parkin* and *PINK1* mutation carriers.

At the molecular level, the Parkin and PINK1 proteins have been shown to act—at least in part—in a common metabolic pathway. The Parkin protein functions as ubiquitin ligase, whereas PINK1 is a mitochondrially localized kinase of as yet largely unknown function. However, an essential pro-mitochondrial function has been demonstrated for both endogenous Parkin and PINK1 proteins in two recent studies analyzing the structural integrity and function of *Drosophila* melanogaster cells that were exposed to high energy demands. While removal of *Drosophila* PINK1 resulted in several loss-of-function phenotypes, including defects in mitochondrial morphology, expression of human PINK1 as well as transgenic expression of Parkin both markedly improved or even restored mitochondrial integrity and other pathologic features.[48,49] This important finding is in keeping with a common intracellular pathway that locates Parkin activity downstream of PINK1 function.[48,49] Given the interactions of the gene products at the cellular level, it comes as no surprise that mutations in either of these genes result in a virtually identical clinical picture in humans. Along the same lines, our results show that two distinct genotypes (i.e., a single mutant allele of the *Parkin* or *PINK1* gene) share an identical morphometric phenotype. The identical morphometric phenotype in asymptomatic mutation carriers suggests that these similarities extend to similar morphometric changes in brain tissue or even similar presymptomatic compensatory mechanisms in heterozygous carriers of *Parkin* and *PINK1* mutations.

REFERENCES

1. Piccini P, Burn DJ, Ceravolo R, Maraganore D, Brooks DJ. The role of inheritance in sporadic Parkinson's disease: evidence from a longitudinal study of dopaminergic function in twins. Ann Neurol 1999;45:577–582.
2. Bezard E, Gross CE, Brotchie JM. Presymptomatic compensation in Parkinson's disease is not dopamine-mediated. Trends Neurosci 2003;26:215–221.
3. Klein C, Schlossmacher MG. Parkinson disease genetics: Implications for neurological care. Nat Clin Neurol 2006;2:136–146.
4. Bonifati V, Rohe CF, Breedveld GJ, et al. Early-onset parkinsonism associated with PINK1 mutations: frequency, genotypes, and phenotypes. Neurology 2005; 65:87–95.
5. Hedrich K, Hagenah J, Djarmati A, et al. Clinical spectrum of homozygous and heterozygous PINK1 mutations in a large German family with Parkinson disease: role of a single hit? Arch Neurol 2006;63:833–838.
6. Klein C, Schumacher K, Jacobs H, et al. Association studies of Parkinson's disease and parkin polymorphisms. Ann Neurol 2000;48:126–127.
7. Abou-Sleiman PM, Muqit MM, McDonald NQ, et al. A heterozygous effect for PINK1 mutations in Parkinson's disease? Ann Neurol 2006;60:414–419.
8. Pramstaller PP, Schlossmacher MG, Jacques TS, et al. Lewy body Parkinson's disease in a large pedigree with 77 Parkin mutation carriers. Ann Neurol 2005;58:411–422.
9. Hilker R, Klein C, Ghaemi M, et al. Positron emission tomographic analysis of the nigrostriatal dopaminergic system in familial parkinsonism associated with mutations in the parkin gene. Ann Neurol 2001;49:367–376.
10. Khan NL, Scherfler C, Graham E, et al. Dopaminergic dysfunction in unrelated, asymptomatic carriers of a single parkin mutation. Neurology 2005;64:134–136.
11. Broussolle E, Lucking CB, Ginovart N, Pollak P, Remy P, Durr A. [18 F]-dopa PET study in patients with juvenile-onset PD and parkin gene mutations. Neurology 2000;55:877–879.
12. Khan NL, Brooks DJ, Pavese N, et al. Progression of nigrostriatal dysfunction in a parkin kindred: an [18F]dopa PET and clinical study. Brain 2002;125: 2248–2256.
13. Scherfler C, Khan NL, Pavese N, et al. Striatal and cortical pre- and postsynaptic dopaminergic dysfunction in sporadic parkin-linked parkinsonism. Brain 2004; 127:1332–1342.
14. Walter U, Klein C, Hilker R, Benecke R, Pramstaller PP, Dressler D. Brain parenchyma sonography detects preclinical parkinsonism. Mov Disord 2004;19:1445–1449.
15. Buhmann C, Binkofski F, Klein C, et al. Motor reorganization in asymptomatic carriers of a single mutant Parkin allele: a human model for presymptomatic parkinsonism. Brain 2005;128:2281–2290.
16. van Eimeren T, Siebner HR. An update on functional neuroimaging of parkinsonism and dystonia. Curr Opin Neurol 2006;19:412–419.
17. Hilker R, Klein C, Hedrich K, et al. The striatal dopaminergic deficit is dependent on the number of mutant alleles in a family with mutations in the parkin gene: evidence for enzymatic parkin function in humans. Neurosci Lett 2002;323:50–54.
18. Hedrich K, Hagenah J, Djarmati A, et al. Clinical spectrum of homo- and heterozygous PINK1 mutations in a large German family with Parkinson's disease: role of a single hit? Arch Neurol 2006;63:833–838.
19. Good CD, Johnsrude I, Ashburner J, Henson RN, Friston KJ, Frackowiak RS. Cerebral asymmetry and the effects of sex and handedness on brain structure: a

voxel-based morphometric analysis of 465 normal adult human brains. Neuroimage 2001;14:685–700.

20. Pavese N, Andrews TC, Brooks DJ, et al. Progressive striatal and cortical dopamine receptor dysfunction in Huntington's disease: a PET study. Brain 2003;126:1127–1135.

21. Tzourio-Mazoyer N, Landeau B, Papathanassiou D, et al. Automated anatomical labeling of activations in SPM using a macroscopic anatomical parcellation of the MNI MRI single-subject brain. Neuroimage 2002;15:273–289.

22. Maldjian JA, Laurienti PJ, Kraft RA, Burdette JH. An automated method for neuroanatomic and cytoarchitectonic atlas-based interrogation of fMRI data sets. Neuroimage 2003;19:1233–1239.

23. Patlak CS, Blasberg RG. Graphical evaluation of blood-to-brain transfer constants from multiple-time uptake data. Generalizations. J Cereb Blood Flow Metab 1985;5:584–590.

24. Rinne OJ, Nurmi E, Ruottinen HM, Bergman J, Eskola O, Solin O. [(18)F]FDOPA and [(18)F]CFT are both sensitive PET markers to detect presynaptic dopaminergic hypofunction in early Parkinson's disease. Synapse 2001;40:193–200.

25. Khan NL, Valente EM, Bentivoglio AR, et al. Clinical and subclinical dopaminergic dysfunction in PARK6-linked parkinsonism: an 18F-dopa PET study. Ann Neurol 2002;52:849–853.

26. Adams JR, van Netten, H Schulzer M, et al. PET in LRRK2 mutations: comparison to sporadic Parkinson's disease and evidence for presymptomatic compensation. Brain 2005;128:2777–2785.

27. Kempermann G, Kuhn HG, Gage FH. More hippocampal neurons in adult mice living in enriched environment. Nature 1997;386:493–495.

28. Corson PW, Nopoulos P, Miller DD, Arndt S, Andreasen NC. Change in basal ganglia volume over 2 years in patients with schizophrenia: typical versus atypical neuroleptics. Am J Psychiatry 1999;156:1200–1204.

29. Mink JW. The basal ganglia: focused selection and inhibition of competing motor programs. Prog Neurobiol 1996;50:381–425.

30. Parent A, Hazrati LN. Functional anatomy of the basal ganglia. I. The cortico-basal ganglia-thalamo-cortical loop. Brain Res Rev 1995;20:91–127.

31. Kotter R, Wickens J. Interactions of glutamate and dopamine in a computational model of the striatum. J Comput Neurosci 1995;2:195–214.

32. Centonze D, Picconi B, Gubellini P, Bernardi G, Calabresi P. Dopaminergic control of synaptic plasticity in the dorsal striatum. Eur J Neurosci 2001;13:1071–1077.

33. Bergman H, Feingold A, Nini A, et al. Physiological aspects of information processing in the basal ganglia of normal and parkinsonian primates. Trends Neurosci 1998;21:32–38.

34. Wichmann T, DeLong MR. Pathophysiology of Parkinson's disease: the MPTP primate model of the human disorder. Ann NY Acad Sci 2003;991:199–213.

35. Bar-Gad I, Morris G, Bergman H. Information processing, dimensionality reduction and reinforcement learning in the basal ganglia. Prog Neurobiol 2003;7:439–473.

36. Nambu A, Tachibana Y, Kaneda K, Tokuno H, Takada M. Dynamic model of basal ganglia functions and Parkinson's disease. In: Bolam JP, Ingham CA, Magill PJ. Advances in Behavioral Biology. The Basal Ganglia VIII. 2005;56:307–312.

37. Levy R, Hutchison W, Lozano AM, Dostrovsky JO. High-frequency synchronization of neuronal activity in the subthalamic nucleus of parkinsonian patients with limb tremor. J Neurosci 2000;15:7766–7775.

38. Raz A, Vaadia E, Bergman H. Firing patterns and correlations of spontaneous discharge of pallidal neurons in the normal and the tremulous 1-methyl-4-phenyl-1,2,3,6-tetrahydropyridine vervet model of parkinsonism. J Neurosci 2000;15:8559–8571.

39. Kuhn A, Kupsch A, Schneider GH, Brown P. Reduction in subthalamic 8-35 Hz oscillatory activity correlates with clinical improvement in Parkinson's disease. Eur J Neurosci 2006;23:1956–1960.

40. Brown P, Williams D. Basal ganglia local field potential activity: character and functional significance in the human. Clin Neurophysiol 2006;117:474–475.

41. Deuschl G, Wilms H. Clinical spectrum and physiology of palatal tremor. Mov Disord 2002;17:63–66.

42. Anderson BJ, Eckburg PB, Relucio KI. Alterations in the thickness of motor cortical subregions after motor-skill learning and exercise. Learn Mem 2002;9:1–9.

43. Kleim JA, Vij K, Ballard DH, Greenough WT. Learning-dependent synaptic modifications in the cerebellar cortex of the adult rat persist for at least four weeks. J Neurosci 1997;17:717–721.

44. Trachtenberg JT, Chen BE, Knott GW, et al. Long-term in vivo imaging of experience-dependent synaptic plasticity in adult cortex. Nature 2002;420:788–794.

45. Draganski B, Gaser C, Busch V, Schuierer G, Bogdahn U, May A. Neuroplasticity: changes in grey matter induced by training. Nature 2004;427:311–312.

46. Draganski B, Gaser C, Kempermann G, et al. Temporal and spatial dynamics of brain structure changes during extensive learning. J Neurosci 2006;26:6314–6317.

47. Lucking CB, Durr A, Bonifati V, et al. Association between early-onset Parkinson's disease and mutations in the parkin gene. French Parkinson's Disease Genetics Study Group. N Engl J Med 2000;342:1560–1567.

48. Park J, Lee SB, Lee S, et al. Mitochondrial dysfunction in Drosophila PINK1 mutants is complemented by parkin. Nature 2006;441:1157–1161.

49. Clark IE, Dodson MW, Jiang C, et al. Drosophila PINK1 is required for mitochondrial function and interacts genetically with parkin. Nature 2006;441:1162–1166.